

High resolution MRI at 21.1 T of the hippocampus and temporal lobe white matter in the differential classification of Alzheimer's Disease and Diffuse Lewy Body Disorder

Parastou Foroutan^{1,2}, Melissa M Murray³, Shinsuke Fujioka⁴, Katherine J Schweitzer⁴, Dennis W Dickson³, Zbigniew K Wszolek⁴, and Samuel Colles Grant^{1,5}
¹Center for Interdisciplinary Magnetic Resonance, The National High Magnetic Field Laboratory, Tallahassee, Florida, United States, ²Imaging, The H. Lee Moffitt Cancer Center, Tampa, Florida, United States, ³Pathology and Neuroscience, The Mayo Clinic, Jacksonville, Florida, United States, ⁴Neurology, The Mayo Clinic, Jacksonville, Florida, United States, ⁵Chemical & Biomedical Engineering, The Florida State University, Tallahassee, Florida, United States

Introduction: The two most common forms of cognitive disorders that induce dementia are Alzheimer's disease (AD) and diffuse Lewy Body disorder (DLBD). Although these conditions differ histopathologically such that AD is associated with amyloid (A β) plaques and neurofibrillary tangles while DLBD is an α -synucleinopathy, clinical similarities make it difficult to distinguish between them. In pathological animal and human tissue [1-3], A β plaques appear to coincide with iron-induced hypointensities observed in T₂- and T₂^{*}-weighted MR images. Similarly, the presence of Lewy bodies, or rather α -synuclein, also has been linked to increases in iron content; however, the underlying pathomechanism for both these findings are yet to be understood [4]. In this work, fixed postmortem sections of human hippocampi diagnosed with AD and DLBD were evaluated using MRI at 21.1 T. Specifically, the samples were analyzed using high resolution 3D datasets, diffusion-weighted imaging and relaxation maps of T₂ and T₂^{*} compared to histology.

Methods: Fixed postmortem specimens harvested from sex- and age matched patients displaying AD (n=13) and DLBD (n=7) were compared to healthy subjects (n=6). The fixed samples were washed in phosphate buffered saline and placed in Fluorinert (FC-43, 3M Corp.) to reduce susceptibility artifacts [5]. MR data were acquired using a 21.1-T, ultra-widebore (105-mm) vertical magnet equipped with a Bruker Avance III console and specially built, 1 T/m/A triple axis gradient system (RRI Inc., Billerica MA) [6,7]. Utilizing a 33-mm birdcage coil, 3D Fast Low Angle Shot (FLASH) images were acquired at an isotropic resolution of 50 μ m over 4.3 hours at 14 °C. T₂^{*}-weighted multiple gradient recalled echo (GRE) and T₂-weighted spin-echo (SE) sequences were acquired over a range of echo times to generate relaxation maps. Multi-slice diffusion-weighted spin echo (DWSE) sequences with four diffusion weightings (b values = 0-1500 s/mm²) also were acquired. For quantitative analysis of T₂, T₂^{*} and signal intensity (SI), separate manually drawn regions of interest (ROIs) were traced over the temporal lobe white matter (TLWM), Parahippocampal gyrus (PHCG), Subiculum (Sub), CA1 and the entire hippocampus (HC). Histology included stains for iron (Prussian Blue, PB) and ferritin-L. Neural density and vacuolization were quantified with hematoxylin & eosin (H&E).

Results & Discussion: High resolution datasets, parametric relaxation maps and regional quantification of T₂ and T₂^{*} provided significant distinctions between healthy and pathological specimens diagnosed with AD or DLBD. With respect to T₂ and T₂^{*}, the largest difference from controls and AD was evaluated for the TLWM while DLBD showed the largest impact on the PHCG. More importantly, the MR related findings of this study, as confirmed by the histological analysis, allowed for the quantitative distinction between AD and DLBD. This data suggests that lower T₂ and T₂^{*} times are correlated with chronic DLBD rather than chronic AD or control sections while increased relaxation values and ADC (not shown) coincide with chronic AD pathology. H&E for vacuolization indicated a larger loss of cells and neuropils in AD compared to both controls and DLBD. While T₂ times correlated with vacuolization in TLWM, PHCG and CA1 and inversely with ferritin in TLWM and CA1, neural cell count did not correlate with either T₂ or T₂^{*}.

In conclusion, this work suggests that it is possible to differentiate quantitatively between neurologically healthy brain tissue and pathological specimens diagnosed with AD or DLBD. Although evaluated at 21.1 T, these quantifiable MR parameters have potential for translation to lower clinical fields and could provide clinicians with the opportunity to differentiate between the two pathologies. Though histological findings correlate well with relaxation and are in agreement with previous research, the relatively low %PB and high %Fer detected in the AD and DLBD cases may indicate brain iron deficiencies that develop in the chronic stages of these pathologies.

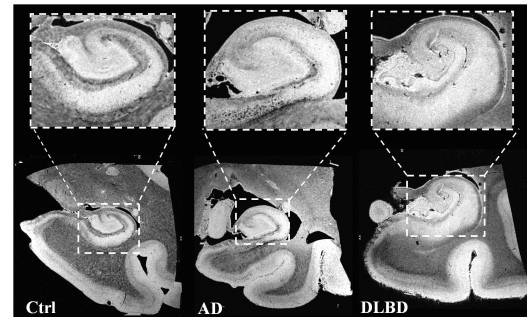


Fig 1. 3D FLASH datasets (iso. res.=50 μ m) of hippocampal sections from a healthy control and tissues diagnosed with AD or DLBD.

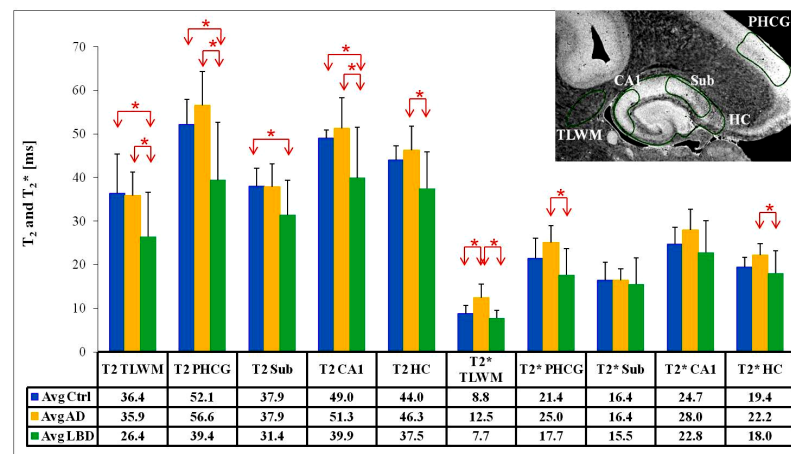
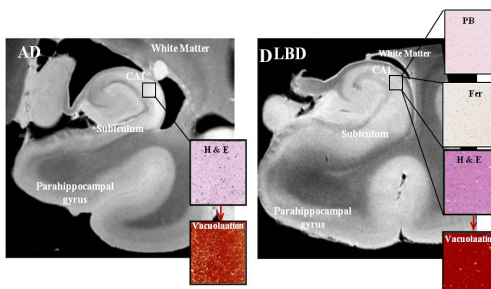


Fig 2. Quantified T₂ and T₂^{*} times displaying the differences between the various groups and in particular the opposite trend between AD and DLBD versus controls. Brackets indicate statistical significance from a one-way ANOVA and LSD test ($p < 0.05$).



ROI	% PB			% Fer		
	Control	AD	DLBD	Control	AD	DLBD
PHCG	0.05±0.03	0.06±0.04	0.04±0.01	3.9±3.5	4.6±0.4	8.1±5.7
Sub	0.04±0.02	0.10±0.06	0.03±0.02	1.9±0.3	3.9±3.4	8.8±3.5
CA1	0.04±0.02	0.08±0.05	0.03±0.01	1.9±0.6	3.1±1.6	9.1±4.7

Fig 3. L: T₂-weighted MSME images overlaid with histological outsets of the CA1 showing H&E for vacuolization in AD and PB, Fer and H&E for vacuolization for DLBD and burden of total iron (%PB) and Ferritin (%Fer). R: Brackets indicate statistical significance in a one-way ANOVA and LSD test ($p < 0.05$).

Acknowledgements & References: MR data was collected at The National High Magnetic Field Laboratory (NHMFL) at The Florida State University. Funding was provided by the NSF (DMR-0084173 and NHMFL User Collaborations Grant Program to SCG).
1. Vanhoutte G *et al.*, (2005), MRM., 53(3). **2.** Chamberlain R *et al.*, (2011), Curr Med Imaging Rev., 7(1). **3.** Meadowcroft M *et al.*, (2009), J MRI., 29(5). **4.** Neumann M *et al.*, (2000), Acta Neuropathol. 100(5). **5.** Schweitzer KJ *et al.*, (2010). Neurology. 74(20). **6.** Fujioka S *et al.*, (2011) Rinsho Shinkeigaku. 51(8). **7.** Fu R *et al.*, (2005) J Magn Reson. 177(1).